Salivary proteins of a gall-inducing aphid and their impact on early gene responses of susceptible and resistant host-plant genotypes

Luis Portillo Lemus [1, 2] *, Jessy Tricard [1, 2] *, Jérôme Duclercq [2], Quentin Coulette [2], David Giron [3], Christophe Hano [1], Elisabeth Huguet [3], Frédéric Lamblin [1], Anas Cherqui [2] °, Aurélien Sallé [1] °

[1] Laboratoire de Biologie des Ligneux et des Grandes Cultures, INRA, Université d'Orléans, 45067, Orléans, France

[2] Ecologie et Dynamique des Systèmes Anthropisés, EDYSAN UMR CNRS-UPJV 7058, Université de Picardie Jules Verne, Amiens, France

[3] Institut de Recherche sur la Biologie de l'Insecte, UMR 7261, CNRS/Université François-Rabelais de Tours, Tours, France

* L. Portillo Lemus and J. Tricard should be considered joint first author

° A. Cherqui and A. Sallé should be considered joint senior author

Funding

This study has been supported by the Région Centre-Val de Loire Project no. 2014 00094521 (InsectEffect) coordinated by D. Giron.

Abstract

Plant manipulation by herbivores requires fine-tuned reprogramming of host metabolism, mediated by effector molecules delivered by the parasite into its host. While plant galls may represent the epitome of plant manipulation, secretomes of gall-inducers and their impact on host-plants have been rarely studied. We characterized, with transcriptomic and enzymatic approaches, salivary glands and saliva of a

gall-inducing aphid, *Phloeomyzus passerinii*. Early responses to aphid saliva of plant genes belonging to different metabolic and signaling pathways were assessed *in vivo*, with poplar protoplasts, and *in planta*, in a heterologous *Arabidopsis* system. Several effectors potentially interfering with plant signaling have been identified, including binding proteins, oxidoreductases, and phosphatidylinositol phosphate kinases. Compatible interactions between protoplasts of a susceptible poplar genotype and the saliva of *P. passerinii* led to an overall downregulation of defense-related genes while an upregulation was observed during both incompatible interactions, with a resistant poplar genotype, and non-host interactions, with the saliva of *Myzus persicae*, an aphid which does not feed on poplars. Compatible interactions affected both auxin transport and homeostasis potentially leading to an intracellular accumulation of auxin, which was further supported by *in planta* assays. Our results support the hypothesis that effectors interfere with downstream signaling and phytohormone pathways.

Keywords

Effector, *Myzus persicae*, *Phloeomyzus passerinii*, plant-insect interaction, *Populus*, resistance, RT-qPCR

Acknowledgements

We thank Léa Fléchon for her assistance with transcriptome analyses.

1 Introduction

Nutritional imbalance and defense mechanisms are major hurdles hampering plant resources exploitation by animals (Schoonhoven, Van Loon, & Dicke, 2005). To cope with this, some herbivores have evolved strategies consisting in remodeling plant tissues to turn them into optimal substrates for their development and fitness (Lieutier et al., 2017). The epitome of such plant manipulation is certainly gall induction, triggering sometimes spectacular and complex tissue reorganization resulting in new plant organs, within which parasites feed and grow (Stone & Schönrogge, 2003; Shorthouse, Wool & Raman, 2005; Giron, Huguet, Stone & Body, 2016). To adapt plant tissues to nutritional requirements of parasites and to circumvent plant defenses, gall development implies fine-tuned metabolism reprogramming, and direct modulations of both primary and secondary metabolisms of host plants have been reported for gall-inducing organisms (Giron et al., 2016). More specifically, since they are important regulators of plant growth, differentiation and defense, phytohormones are classical targets of plant-manipulating organisms, and considered key factors intimately involved in the success or failure of gall differentiation (Tooker & Helms, 2014; Giron et al., 2016).

Host metabolism hijacking by plant-manipulating organisms is considered to be mediated by effector molecules delivered into the host-plant (Hogenhout & Bos, 2011; Giron et al., 2016). Effector proteins secreted by herbivores in general have various functions, including suppression of plant defense, alteration of plant development, and manipulation of plant resources (Hogenhout & Bos, 2011; Giron et al., 2016). For gall-inducing organisms, similar functions are expected, especially disruption or diversion of hormone-dependent pathways (Tooker & Helms, 2014) and inactivation of second messengers involved in stress signaling like Ca^{2+}, reactive oxygen species (ROS) and extracellular ATP for instance (Will, Tjallingii, Thönnessen & van Bel, 2007; Guiguet et al., 2016). While there is a growing literature dealing with the identification of these effectors in herbivores, like aphids (e.g. Harmel et al., 2008;

Nicholson, Hartson & Puterka, 2012; Vandermoten et al., 2014; Boulain et al., 2018), few investigations have been performed on secretions of gall-inducing organisms, with notable exceptions of the Hessian fly (*Mayetiola destructor*, Say) and root-knot nematodes (*Meloidogyne* spp.) for instance (e.g. Zhao et al., 2015; Favery, Quentin, Jaubert-Possamai & Abad, 2016). So far, the Hessian fly is the only gall-inducing insect with a sequenced genome, and whose salivary gland transcriptome and proteome have been studied (Stuart, Chen, Shukle & Harris, 2012; Zhao et al., 2015). Candidate genes with effector functions have been detected and gene-for-gene interaction between insect strains and host-plant genotypes has been demonstrated (Stuart et al., 2012; Zhao et al., 2015; 2016). How these effectors contribute to gall induction is still unclear, but it is hypothesized that they interfere with downstream signaling and phytohormone pathways (Zhao et al., 2016).

To validate the relevance of candidate effectors for plant-insect interactions, several approaches have been used. *In planta* modulation of candidate effectors expression allowed to highlight impacts of effector proteins on physiological traits and behavior of insects and plant responses (e.g. Mutti et al., 2008; Atamian et al., 2013; Zhao et al., 2016). Alternatively, direct applications of oral secretions and saliva infiltration into host plants also gave conclusive results (e.g. De Vos & Jander, 2009; Chaudhary, Atamian, Shen, Briggs & Kaloshian, 2014). Nonetheless, probably because of their complex life cycles and generally concealed endophytic development, very few functional validation experiments have been performed with gall-inducing insects (e.g. Zhao et al., 2016). In-depth functional molecular approaches would allow to unravel the mechanisms that contribute to plant manipulation by these organisms and could possibly lead to identification of convergent mechanisms among them (Giron et al., 2016).

Here, we report the characterization of salivary proteins of *Phloeomyzus passerinii* Sign., a gall-inducing aphid colonizing poplars (Sallé, Pointeau, Bankhead-Dronnet, Bastien & Lieutier, 2017). As this insect can be easily handled under laboratory conditions, and its saliva can be collected on artificial medium, we performed innovative functional validation assays to address the impact of the saliva of a gall-inducing

90 organism on gene responses of its host-plant. Our objectives were (i) to characterize with transcriptomic
91 and enzymatic approaches the salivary glands and saliva, respectively, of *P. passerinii*, (ii) to assess *in*
92 *vivo*, with a RT-qPCR approach, early responses of poplar genes belonging to different metabolic and
93 signaling pathways using protoplasts exposed to aphid saliva, and (iii) to investigate the impact of
94 salivary extracts on specific gene expression *in planta*, in a heterologous *Arabidopsis* system. For all these
95 steps comparative approaches have been used. The determined salivary proteins of *P. passerinii* were
96 compared with those of a sap-feeding aphid *Myzus persicae* (Sulzer) (Harmel et al., 2008; De Vos &
97 Jander, 2009) in order to identify proteins common to both aphid species as well as proteins specific to *P.*
98 *passerinii*. To get insight into how *P. passerinii* manipulates host metabolism and stress responses to
99 perform gall-induction, the impact of salivary extracts on gene expression has been assessed with poplar
100 genotypes either susceptible or resistant to *P. passerinii*, i.e. during compatible and incompatible
101 interactions, respectively. These poplar genotypes have also been exposed to salivary extracts of *M.*
102 *persicae*, which led to non-host interactions since *M. persicae* does not feed on poplar.
103
104 ## 2 Materials and Methods
105
106 ### 2.1 Plant and insect material
107 *Phloeomyzus passerinii* is a specialist of poplars, inducing open galls in the cortical parenchyma of its
108 host-trees and feeding on cell contents (Pointeau et al., 2012; Dardeau et al., 2014; Sallé et al., 2017).
109 During gall induction in susceptible hosts, cell multiplication in cortical parenchyma is visible one week
110 after the onset of aphid probing, and three weeks later thin-walled hypertrophied cells differentiate
111 while vacuolar phenolic compounds disappear from the galled tissues (Dardeau et al., 2014). In resistant
112 host genotypes, lignin, tannins and flavanols accumulate at the probing site one week after the onset of
113 probing and no gall differentiation occurs subsequently. As a consequence, *P. passerinii* cannot develop

on these genotypes (Dardeau et al., 2014). All individuals of *P. passerinii* used either for transcriptomic analyses of salivary glands or saliva collection originated from the same monoclonal colony established from an apterous parthenogenetic female, collected in 2013 in Brézé (France). The colony was maintained in the laboratory on potted stem cuttings of I-214, a *Populus x canadensis* Moench. genotype, under 20 ± 1 °C, 70 ± 10% relative humidity and 16/8 h light/dark cycles. The green peach aphid, *Myzus persicae* is a sap-feeder and a generalist aphid. Nonetheless, its host range does not include poplars, and preliminary establishment attempts confirmed that it cannot settle and develop on poplars (data not shown). Therefore non-host interactions are expected between this aphid species and poplar genotypes. Individuals of *M. persicae* originated from a monoclonal colony established from an apterous parthenogenetic female collected in 1999 on a potato plant in Loos-en-Gohelle (France). The colony was maintained under the same controlled conditions as *P. passerinii*, on turnips (Vilmorin).

For the protoplasts production, stem-cuttings of two *P. x canadensis* genotypes commonly planted in France, I-214 and Koster, were used for the experiments. I-214 is highly susceptible to *P. passerinii*, whereas aphids cannot settle on Koster which is consequently considered to be highly resistant to *P. passerinii* (Sallé et al., 2017). Consequently, compatible and incompatible interactions are expected between *P. passerinii* and I-214 and Koster, respectively, and non-host interactions should take place between *M. persicae* and both poplar genotypes. Stem cuttings (ca. 25 cm long, 2 cm diameter) were provided by the experimental nursery of Guéméné-Penfao (France). They were collected in the autumn of 2016, and kept at 2°C, in dry conditions until use. In January 2017, the stem-cuttings were removed from storage and planted in 0.4 L pots, filled with a sterile sand-compost (50:50) mixture (Klasmann substrate 4 no. 267). The cuttings were then transferred to a growth chamber (20 ± 1°C, 70 ± 10% relative humidity, 16/8 h light/dark photoperiod, 2.65 kLx, and watered three times a week).

For *in planta* functional validation of the effects of salivary proteins, two *Arabidopsis thaliana* (L.) Heynh. transgenic lines were used, the auxin-responsive reporter *pIAA2*::GUS (Bishopp et al., 2011) and the cytokinins-responsive reporter *pARR16*::GUS (European Arabidopsis Stock Centre). Seeds were sterilized with chloral gas, sown in Petri dishes on 0.8% (w/v) agar with 1% (w/v) sucrose-containing 0.5 Murashige and Skoog medium (MS), stored for 2 days at 4°C, and grown on vertically oriented plates in growth chambers under a 16/8 h light/dark photoperiod at 18°C.

2.2 Salivary transcriptome

2.2.1 Sample collection, RNA isolation and *de novo* transcriptome assembly

About 500 adults of apterous parthenogenetic *P. passerinii* aphids were dissected to collect pairs of salivary glands. Total RNA was extracted using the GeneJET RNA Purification kit (Thermo Fischer Scientific), according to manufacturer's instructions. RNA was DNase treated using RNase-Free DNase Set (Qiagen). RNA concentration was measured using the Qubit® RNA Assay Kit (Life Technologies) and a Qubit® 2.0 Fluorometer (Invitrogen). Construction of cDNA-library and sequencing were performed by Eurofins® Genomics using a MiSeq v3 Reagent Kit (600 Cycles PE, Illumina, USA) and a MiSeq sequencer (Illumina). For the *de novo* transcriptome assembly, 15,453,942 pair-ended reads were sequenced and assembled using Velvet (v1.2.10; Zerbino & Birney, 2008) and Oases (v0.2.8; Schulz, Zerbino, Vingron & Birney, 2012) software tools (table S1). A multi-kmer approach was applied. Separate assemblies with different kmer lengths have been conducted and the individual assemblies have been merged to a final assembly. Kmer lengths of 69, 89, 109 and 129 were used. The separate assemblies were merged following the filter1-CD-HIT-EST procedure proposed in Yang & Smith (2013). This Transcriptome Shotgun Assembly project has been deposited at DDBJ/EMBL/GenBank under the accession GHDF00000000. The version described in this paper is the first version, GHDF01000000.

161

162 2.2.2 Annotation, secreted proteins detection and identification

163 To perform comparisons with *M. persicae* the transcriptome of this aphid was retrieved on NCBI
164 (http://www.ncbi.nlm.nih.gov/genbank/, accession numbers: DW010205 - DW015017, EC387039 -
165 EC390992, EE570018 - EE572264, EE260858 - EE265165, ES444641 - ES444705, ES217505 - ES226848,
166 and ES449829 - ES451794). Salivary transcriptomes have been annotated using the pipeline described in
167 figure S1. Transcripts were first translated into amino acid sequences using Prodigal (v2.5; Hyatt et al.
168 2010). We then used the SignalP 4.0 Server (v4.1) to predict the presence of signal peptides and cleavage
169 sites in the amino acid sequences (Petersen, Brunak, von Heijne & Nielsen, 2011). To predict
170 transmembrane domains, we submitted each amino acid sequence with a signal peptide to the TMHMM
171 Server (v. 2.0; Ji et al., 2013). Putative proteins with a signal peptide and no transmembrane domain
172 were considered to be potential secreted proteins. The sequences of complete ORFs without signal
173 peptide were analyzed again with SecretomeP (v2.0; Bendtsen, Jensen, Blom, von Heijne & Brunak,
174 2004). To remove mitochondrial proteins with a signal peptide, which are not secreted in the saliva,
175 sequences were analyzed with TargetP (v1.1; Emanuelsson, Nielsen, Brunak, & von Heijne, 2000).
176 Likewise, to remove proteins of the endoplasmic reticulum with a signal peptide, sequences were
177 analyzed with PS-scan (Prosite pattern: PS00014), and with PredGPI (Pierleoni, Martelli & Casadio, 2008)
178 for glycosylphosphatidylinositol-anchor signals.
179 The remaining proteins were first mapped against the non-redundant protein sequences (nr) using
180 Blastp (v2.3.0, NCBI, accessed on 03/30/2016), with an E-value cutoff at 1^{e-3}. Protein domains were
181 annotated with Blast2Go (v3.3; Conesa et al., 2005), and InterProScan (v5.30-69; Jones et al., 2014).
182 Whenever possible, protein sequences were assigned to Gene ontology (GO) terms with an E-value
183 cutoff at 1^{e-6}, enzyme codes (EC) and KEGG pathways.

184 OrthoVenn (http://aegilops.wheat.ucdavis.edu/OrthoVenn; Wang et al., 2015) has been used to identify
185 orthologous proteins within and between salivary transcriptomes of the two aphids. Intraspecific
186 orthologous proteins are first grouped into clusters, which are then compared between species. Each
187 cluster has been annotated with the Uniprot database (http://www.uniprot.org; Pundir, Martin &
188 O'Donovan, 2017) and the nr peptide sequence database (NCBI, accessed on 03/30/2016).
189 To detect proteins orthologous to salivary effectors of aphids, protein sequences of known aphid
190 effectors, i.e. C002, ACE1, ACE2, ACYPI39568, ACYPI00346, MpC002, Mp1, Mp2, Mp42, Mp55, Me10,
191 Me23 (Guo et al., 2014; Jaouannet et al., 2014; Pan, Zhu, Luo, Kang & Cui, 2015), have been compared to
192 the salivary transcriptome of *P. passerinii* with Blastp (E-value ≤ 1^{e-3}).
193
194 2.3 Functional validation assays
195
196 2.3.1 Aphid saliva collection
197 Aphids secrete two types of saliva within their host-plants, liquid and solid saliva (Will, Steckbauer, Hardt
198 & van Bel, 2012). The solid saliva is secreted during probing. It hardens rapidly and forms a solid sheath
199 encasing aphid stylets within the host-plant, while the liquid saliva is secreted within cells and sieve
200 tubes (Will et al., 2012). Both types of saliva contain effectors (e.g. Will et al., 2012; Elzinga & Jander,
201 2013), and have been collected in our experiments. Because of the particular trophic substrates of *M.*
202 *persicae* and *P. passerinii* (i.e. sap and galled tissues, respectively), a special protocol has been used for
203 each species. The saliva of *P. passerinii* was collected after incubation of 30 to 40 individuals of 2nd and
204 3rd instars aphids on sachets of Parafilm© membranes containing an artificial diet (Cherqui & Tjallingii,
205 2000). The artificial diets were constituted by a disc of 0.5% (w/v) agar completed with 150 µL of 15%
206 (w/v) sucrose. The saliva of *M. persicae* was collected after incubation of 30 to 40 individuals, of 3rd and
207 4th instars, on artificial diet containing 120 µL of a 15% (w/v) sucrose as previously described by Cherqui

& Tjallingii (2000). Aphids were deposited in a feeding chamber during 24 h at 20°C, 60 ± 1% relative humidity and a 16/8 h light/dark period with 2.65 kLx. Feeding chambers containing the artificial diets, incubated in the absence of aphids, were used as control samples.

For *P. passerinii*, after 24 h aphid salivation, artificial diet discs were collected and transferred into 100 µL of TE buffer (10 mM Tris, 1 mM EDTA, pH 8). The salivary proteins were released from the artificial diet according to Yang et al. (2010), with slight modifications. The tubes containing artificial diet discs were frozen in liquid nitrogen for 1 min, immediately thawed at 70°C for 3 min and then centrifuged at 11,000 x *g* for 20 sec. To discard the excess of agar, salivary extracts were centrifuged in Sartorius tubes with filters of 0.22 µm. The supernatant containing salivary proteins of *P. passerinii* were collected, pooled and then stored at -20°C. For *M. persicae,* after 24 h salivation, aphid saliva was collected according to Harmel et al. (2008). The artificial diet is collected containing soluble saliva. The solid saliva was collected during the rinsing of each lower Parafilm membrane with TE buffer containing 0.1% (w/v) of Tween 20 (TE/Tween). The extracts were centrifuged at 10,000 x *g* for 15 min. The salivary proteins in the pellet were collected, pooled with the soluble saliva and then stored at -20°C.

The sample containing protein saliva extracts were concentrated using 2 mL Vivaspin© tube (Sartorius) with 3kDa cut-off. The tubes were then centrifuged at 5,000 x *g* for 70 to 120 min according to sample volumes, and proteins adhering to membranes were recovered by 100 µL of TE/Tween buffer. Control samples were prepared with artificial diets from feeding chambers without aphids. The protein quantification was performed by measuring absorbance at 280 nm with the NanoDrop© 1000 (ThermoScientific).

2.3.2 Enzyme activities

Several enzyme substrates were added to the previously described artificial diets with or without agarose to detect enzymatic activities present in saliva excreted from the aphid. To visualize proteins in

232 the salivary sheaths, the lower Parafilm© membranes were stained by adding a drop of 0.01% (w/v)
233 Coomassie blue in 10% (v/v) glycerol for 2 h. Dihydroxyphenylalanine (DOPA), 0.1% (w/v) was added to
234 identify phenoloxidase activity (PO; catechol oxidase, EC 1.10.3.1). The enzymatic product, melanin,
235 should stain salivary sheaths and halos around the sheaths. To detect peroxidase (EC 1.11.1.7) activity,
236 artificial diets were immersed for some minutes in 0.1% (w/v) diaminobenzidine (DAB, Sigma) in 50 mM
237 Tris (pH 7.5) containing 0.1% (v/v) H_2O_2 (Sigma). The enzymatic product should induce reddish staining of
238 salivary sheaths and halos. For identification of pectinase activity, 0.1% (w/v) of pectin (Sigma) was
239 added to the medium. After exposure to aphids, the gel was transferred for 3 h into a Petri dish
240 containing 50 mM citrate-phosphate buffer, at pH 5.0 to detect pectin (methyl) esterase (PME, EC
241 3.1.1.11) and at pH 6.4 to detect polygalacturonase (PG, EC 3.1.1.15). The gel was then stained with a
242 solution of 0.01% (w/v) ruthenium red (Sigma) for 1 h, and then washed several times with distilled
243 water. At pH 6.4, red halos around the salivary sheaths indicate PME activity, while non-staining halos at
244 pH 5 in the pink pectin indicate PG activity. Finally, for proteinase activity (EC 3.4.99), 0.5% (w/v) of
245 gelatin (Sigma) was added to the medium. After exposure to aphids, the medium was incubated
246 overnight in a solution of 50 mM Tris (pH 8) containing 100 mM NaCl and 10 mM $CaCl_2$, then stained with
247 Coomassie blue. An absence of blue staining shows proteinase activity. All observations of proteins and
248 enzymatic activities were performed by light microscopy (Axioplan 2, Zeiss, Jena, Germany).
249
250 2.3.3 Poplar protoplast preparations and treatments
251 Mesophyll protoplasts of the two poplar genotypes were obtained from young leaves as described in Wu
252 et al. (2009). Leaves were cut into 1–2 mm fine strips in 0.3 M sorbitol and 66.67 mM $CaCl_2$ (pH 5.6) and
253 lysed in an enzyme solution (0.6 M mannitol, 0.25% (w/v) cellulase Onozuka R-10, 0.05% (w/v)
254 macerozyme R-10) in the dark for 16 h with gentle shaking (30 rpm) at room temperature. Protoplasts
255 were collected by filtering the lysis solution through a 70 µm cell strainer (Falcon®) and concentrated by

spinning down at ≈ 800 x *g* for 10 min at 4 °C. The pellet was washed twice with W5 buffer (154 mM NaCl, 125 mM $CaCl_2$, 5 mM KCl, 5 mM glucose, 0.03% (w/v) MES, pH 5.8) and then resuspended in 0.6 M mannitol to a final concentration of 1×10^6 protoplasts per mL. Protoplasts (1.10^6) were incubated at 20°C with gentle shaking (40 rpm) for 3 h with aphid salivary proteins or with protein extraction buffer (control). Preliminary experiments investigating expression of 10 poplar genes, and conducted with 1, 10, 20, 40 or 80 µg of salivary proteins, indicated that the optimal response (i.e. the maximum fold change) was observed with 1 and 10 µg of salivary proteins of *P. passerinii* and *M. persicae*, respectively. Protoplast viability, before and after treatment with aphid saliva, was assessed using 0.005% (w/v) fluorescein diacetate (FDA). After 5 min of incubation protoplasts were observed under blue light epifluorescence, and cell viability was estimated as the percentage of fluorescent cells. Most protoplasts were intact and viable after enzymatic digestion with cellulase and macerozyme (98%), as well as after incubation with salivary proteins (95%; Fig. S2).

2.3.4 Quantitative RT-PCR

After the aphid saliva treatments, protoplasts were centrifuged at ≈ 800 x *g* for 2 min. Total RNAs were extracted with the RNeasy® Plant Kit Mini Kit (Qiagen). A DNase treatment with the RNase-free DNase Set (Qiagen) was carried out for 15 min at 25°C. Total RNA concentration was determined using a Nanodrop ND-1000 spectrophotometer. All RNA samples were rejected if they did not reach a minimum concentration of 100 ng μL^{-1}, a 260 nm/280 nm ratio between 1.8 and 2.0. Poly(dT) cDNA was prepared from 1 µg total RNA using the iScriptTMcDNA Synthesis Kit (Bio-Rad) and quantified with a LightCycler 480 (Roche) and SYBR GREEN I Master (Roche), according to the manufacturer's instructions. PCR was carried out in 384-well optical reaction plates heated for 10 min to 95°C to activate hot start Taq DNA polymerase, followed by 40 cycles of denaturation for 60 sec at 95°C and annealing/extension for 60 sec at 58°C. The distribution of the quantitative RT-PCR mix containing SYBR Green I Master (Roche), cDNAs

and primers was performed using the EVO150© (Tecan) pipetting robot in a 384-well plate. The expression of 43 genes, belonging to eight different physiological processes or metabolic pathways (i.e. auxin, cytokinins, jasmonates, ethylene, salicylic acid, phenolic compounds, reactive oxygen species (ROS), cell cycle), was quantified with specific primer pairs designed by Quant-Prime (Arvidsson, Kwasniewski, Riaño-Pachón & Mueller-Roeber, 2008) based on the *Populus trichocharpa* sequence (v3.0) from Phytozome (https://phytozome.jgi.doe.gov/pz/portal.html; Table S2). Expression levels were normalized to the levels of *PtUBIQUITIN10* (*PtUBQ10*), commonly used as a reference gene in plants (e.g. Tong, Gao, Wang, Zhou & Zhang, 2009). All RT-qPCR experiments were done with three independent biological replicates, with two technical replicates each. One of the biological replicates of the *M. persicae* – Koster interaction has been excluded from the analyses because of technical issues during quantification. Relative gene expression was calculated according to the $^{\Delta\Delta}$Cp method, with protoplasts incubated with protein extraction buffer as controls. Primers used for gene expression analysis are listed in Table S2.

2.3.5 Histochemical analysis of GUS activity

Transgenic seedlings of *A. thaliana* (five-day-old and eight-day-old for *pIAA2*::GUS and *pARR16*::GUS, respectively) were incubated with 2 mL of liquid MS containing 1 µg and 10 µg of aphid salivary proteins (in TE/Tween buffer) of either *P. passerinii* or *M. persicae* for 3 h and 4 h for *pIAA2*::GUS and *pARR16*::GUS, respectively. Positive controls were incubated with 20 µM of indole acetic acid (IAA) (Sigma-Aldrich), and 20 µM of 6-benzylaminopurine (BAP) (Sigma-Aldrich). Negative controls were incubated in liquid MS and corresponding volumes of TE/Tween buffer. Five seedlings were used for each modality. Seedlings were then incubated in reaction buffer containing 0.1 M sodium phosphate buffer (pH 7), 2 mM ferricyanide, 2 mM ferrocyanide, 0.1% (v/v) Triton X-100 and 1 mg ml^{-1} X-Gluc for 1 up to 24 h in dark at 37 °C. Afterwards, chlorophyll was removed by destaining in 70% ethanol and

304 seedlings were cleared as described by Malamy and Benfey (1997). GUS expression was monitored by
305 differential interference contrast microscopy.
306
307 2.4. Data analysis
308 All tests were carried out with the statistical software R 2.11.0 (R Development Core Team, 2013). RT-
309 qPCR results have been expressed as fold-changes in gene expression compared to the reference gene
310 *PtUBQ10*. Fold-changes have been $\log_2$ - transformed. Following this transformation, fold-changes varied
311 between $-\infty$ and $+\infty$, with negative values corresponding to gene underexpression, positive values to
312 overexpression and zero, to no change in gene expression. Permutational multivariate anovas
313 (permanovas), using 1000 permutations, were computed to test the effect of aphid species and host
314 plant genotype on the simultaneous fold-changes in gene expression of the 43 considered poplar genes
315 using the R package vegan (Oksanen et al. 2013). To visualize similarities and differences in fold-changes
316 a heatmap was built, with genes in columns and modalities in lines. The heatmap was built with a Z-
317 score, i.e. $\log_2$ – transformed fold changes which have been normalized and centered per column.
318 Hierarchical clustering with Euclidean distances was added to the heatmap to visualize the proximity
319 among genes in columns and among modalities in lines.
320 A univariate model has also been used to analyze the effect of modalities (i.e. aphid species and host
321 genotype) on fold-changes of each gene. The model equation was:

$$\log_{10}(y_{ij}) = \alpha_i + \varepsilon_{ij}$$

322 where y_{ij} is the fold-change for the modality i and the biological replicate j, and α_i is the effect of the
323 modality i on relative gene expression. The model error follows a normal distribution, with a null mean
324 and a variance σ^2. There is no intercept in this model and 4 independent α_i parameters were estimated,
325 corresponding to each aphid – poplar genotype combination. These parameters were estimated with a
326 Bayesian approach, with $\alpha_i \sim N(0, 0.5^2)$ for prior. The parameters have been estimated with a Markov

Chain Monte Carlo algorithm and the package R brms (Buerkner, 2016). The maxima *a posteriori* and 95% credibility intervals were calculated, with downregulation and upregulation probabilities for each gene. A credibility interval excluding 1 (i.e. the constitutive expression of genes) indicates a significant effect of aphid saliva on gene expression. This approach was selected because it allows to perform statistical analyses with a limited number of biological replications.

3 Results

3.1 Annotation, secreted proteins detection and identification

From 36,312 and 3,233 transcripts, 1,243 and 221 transcripts were predicted to encode for secreted salivary proteins in *P. passerinii* and *M. persicae*, respectively. About half of them (604) have been annotated for *P. passerinii* and 190 for *M. persicae*. Using OrthoVenn, 121 and 58 protein clusters have been identified for *P. passerinii* and *M. persicae*, respectively. About 17% of these clusters were common between the two aphids (Table S3).

Blast2GO determined that *P. passerinii* salivary proteins were predominantly binding proteins and enzymes (Fig. 1, table S4). The most common enzymes were peptidases (especially serine-type and cysteine-type endopeptidases), kinases (especially phosphatidylinositol phosphate (PIP) kinases) and hydrolases. Several enzymes involved in the degradation of carbohydrates (i.e. cellulase, trehalase, β-glucuronidase, mannosidase and glucosylceramidase), and of phenolic compounds (i.e. peroxidase and oxidoreductase) were also identified (Fig. 1, table S4). Among binding proteins, dimerization protein, nucleic acids binding (especially DNA binding), nucleotide binding (especially ATP binding) and cation-binding (mostly calcium ion-binding and zinc-binding proteins) were the most commonly found (Fig. 1, table S4). Proteins related to hormone activity were also identified. Glucose dehydrogenases were also

detected with OrthoVenn (table S3). Among the 12 aphid salivary effectors considered, five were identified in *P. passerinii*, with low E-values (< 7 e^{-71}): Mp10, ARMET, ACE 1, ACE2 and ACE3.

3.2 Enzyme activities

Staining with Coomassie blue confirmed the protein nature of the salivary sheath material (Fig. 2A) and DOPA staining indicated a phenoloxidase activity in the sheaths (Fig. 2B). Black halos were also observed around some sheaths (Fig. 2B). Likewise, peroxidase activity was found in salivary sheaths and halos around sheaths (Fig. 2C). However, no pectinesterase, polygalacturonase and proteinase activity was detected.

3.3 Quantitative RT-PCR

The multivariate analysis based on the expression of the 43 genes showed a highly significant effect of aphid species (pseudo-$F_{1, 10}$ = 12.07, P < 0.001), no effect of poplar genotype, but a significant aphid x poplar genotype interaction (pseudo-$F_{1, 10}$ = 3.51, P = 0.038). This indicated that the salivary proteins effect differed depending on aphid x poplar genotypes combinations. Fold changes across modalities are presented in figure 3. The hierarchical clustering of modalities (left dendrogram) shows an arrangement of modalities into two groups. In the upper group, most poplar genes were upregulated following incubation with salivary proteins, while in lower group most genes were downregulated (Fig. 3). The upper group gathered most biological replicates of incompatible (i.e. *P. passerinii* – Koster) and non-host (i.e. *M. persicae* – Koster, *M. persicae* – I-214) interactions. The lower group gathered all replicates of compatible interactions (i.e. *P. passerinii* – I-214) and an incompatible one. The hierarchical clustering of genes (upper dendrogram) showed that genes could also be arranged into two groups. The group on the left allowed to separate the effect of salivary proteins of *M. persicae*, with a general downregulation of genes, from those of *P. passerinii*, with a general upregulation (Fig. 3). The group on the right allowed to

374 separate compatible interactions, with a general downregulation of genes, from other interactions
375 during which genes were generally upregulated (Fig. 3). There was no clustering of genes according to
376 physiological process or metabolic pathway.
377 For the auxin pathway, the compatible interaction was characterized by a downregulation of genes
378 related to auxin transport (i.e. *PtAUX1* and *PtPIN1* with downregulation probabilities of 62% and 86%,
379 respectively) and homeostasis (i.e. *GH3* with a downregulation probability >99%; Fig. 4A). However,
380 there was no effect on genes involved in auxin biosynthesis (i.e. *PtNIT1* and *PtYUCCA*). Reverse variations
381 were observed for non-host and incompatible interactions which led to an upregulation of *PtGH3*, with
382 upregulation probabilities >99% for *M. persicae* and 86% for *P. passerinii*, and upregulations of genes
383 related to auxin transport with probabilities always higher than 86% (Fig. 4A).
384 For the cytokinin pathway, the compatible interaction did not affect the expression of genes related to
385 cytokinin metabolism (i.e. *PtLOG5* and *PtIPT*), but downregulated cytokinin signaling genes (*PtAHK4* and
386 *PtARR2*), with downregulation probabilities >99% (Fig. 4B). Non-host interactions led to upregulations of
387 all genes but *PtLOG5*, with probabilities >95% (Fig. 4B). Response of genes to the incompatible
388 interaction followed a similar trend, with upregulation of all genes, including *PtLOG5*, with probabilities
389 >95%.
390 Regarding biotic stress signaling (i.e. jasmonates, salicylic acid, ethylene and ROS), the compatible
391 interaction was characterized by null or downregulation responses for all the considered genes (Fig. S3).
392 For ROS genes weak downregulations were also observed for non-host interactions (>85% and >64%
393 downregulation probabilities for *PtSOD* and *PtCAT*, respectively) and a weak upregulation for the
394 incompatible interaction (91% and 77% upregulation probabilities for *PtSOD* and *PtCAT*, respectively).
395 For salicylic acid, jasmonates and ethylene, non-host interactions induced a strong upregulation of most
396 genes (>99% upregulation probabilities in most cases), except *PtPR5* for salicylic acid which was
397 downregulated (>98% downregulation probabilities), *PtAOS* for jasmonates and *PtEIN2* for ethylene

398 which did not respond. The incompatible interaction resulted in an upregulation of all genes involved in
399 jasmonates and ethylene pathways but to a lesser extent than non-host interactions (>81% upregulation
400 probabilities), except *PtJAZ1* which was downregulated (73% downregulation probability) and *PtJAR1*,
401 *PtERF1* which were not affected. For salicylic acid, weak upregulations were observed for *PtNPR1*, *PtPR5*
402 and *PtNDR1* (>62% upregulation probabilities), and no effect was detected for *PtPR1* and *PtEDS1*.
403 For genes involved in the phenolic compounds pathway, *PtF5H* and *PtANT* were downregulated during
404 the compatible interaction (>85% downregulation probability), while all genes were upregulated during
405 non-host and incompatible interactions (>89% upregulation probability in all cases; Fig. S3). Finally,
406 regarding genes involved in cell cycle, *PtCYCD5*, *PtMCM2* and *PtRBR* tended to be downregulated during
407 compatible interactions (>72% downregulation probability). Conversely, most genes, except *PtCAK1* and
408 *PtMCM2*, were upregulated during non-host interactions (>94% upregulation probabilities in most
409 cases), and most genes were not affected during incompatible interactions, except *PtCDK5*, *PtCDK20* and
410 *PtCAK1* which were upregulated (>95% upregulation probabilities; Fig. S3).
411
412 3.4 Histochemical analysis of GUS activity
413 Salivary proteins of *P. passerinii* increased *pIAA2*::GUS signals (Fig. 5E, 5F, 5I, 5J), which were similar to
414 those caused by an exogenous application of auxin (Fig. 5A and 5B). Incubation with salivary proteins of
415 *M. persicae* resulted in faint colorations (Fig. 5G, 5H, 5K, 5L), similar to those of negative controls (Fig. 5C
416 and 5D).
417 Positive controls of *pARR16*::GUS were characterized by a strong staining in the middle part of root
418 central cylinder (Fig. 6A and 6B), which was weak in negative controls as well as with *M. persicae* salivary
419 proteins (Fig. 6G, 6H, 6K, and 6L). No coloration was visible in the roots of seedlings incubated with
420 salivary proteins of *P. passerinii* (Fig. 6E, 6F, 6I and 6J).
421

4 Discussion

Plant manipulation by parasites requires a finely tuned reprogramming of host metabolism, achieved through secretion of effectors into the host plant (Hogenhout & Bos, 2011; Giron et al., 2016). Using both *in vivo* and *in planta* approaches, we confirmed that salivary proteins impact gene transcription of its host tree, strongly suggesting they mediate the interactions between *P. passerinii* and its host-tree. Salivary extracts of *P. passerinii* significantly affected gene expression of the two host-plant genotypes considered, in a markedly different way. Compatible interactions were characterized by a general trend of gene downregulation in all the metabolic pathways and physiological processes investigated, including genes involved in biotic stress signaling. This supports the hypothesis that the saliva of *P. passerinii* includes effectors proteins affecting plant signaling and defense mechanisms.

Several of the detected salivary proteins may interfere with plant signaling. PIP kinases were quite common in the saliva of *P. passerinii*, but have not been previously reported from any aphid saliva. These enzymes catalyze phosphorylation of phosphatidyl-inositol into phosphatidylinositol-4-5-biphosphate (PIP_2). Hydrolysis of PIP_2 produces secondary messengers like diacylglycerol and inositol-1-4-5-triphosphate (IP_3), which can in turn be hydrolyzed into phosphatidic acid (PA), considered an important signaling molecule in plants, triggered in response to various biotic and abiotic stresses (Testerink & Munnik, 2005). Likewise, PIP_2 and IP_3 can affect cellular oscillations of Ca^{2+} and are involved in multiple processes including cell cycle and phytohormone regulation (Xue, Chen & Mei, 2009). Other proteins, frequently detected in the saliva of *P. passerinii*, may also interfere with secondary messengers like calcium-binding, ATP-binding, and GTP-binding proteins or with hormone signaling like hormone-binding proteins (Vandermoten et al., 2014; Giron et al., 2016). Likewise, it has been hypothesized that trehalase may interfere with trehalose-based defense responses in *A. thaliana* (Nicholson et al., 2012), and

446 cellulases may also contribute to the degradation of oligogalacturonides involved in damage signaling
447 pathways (Cherqui & Tjallingii, 2000). Nucleic acid-binding proteins and protein-binding proteins could
448 also participate in the manipulation of host-plant metabolism (Vandermoten et al., 2014). Finally,
449 oxidoreductases, especially peroxidases and phenoloxidases could degrade phenolic compounds of the
450 host plant (Cherqui & Tjallingii, 2000; Carolan, Fitzroy, Ashton, Douglas & Wilkinson, 2009). Gall
451 induction by *P. passerinii* in susceptible host genotypes is characterized by transient accumulation of
452 phenolic compounds (Dardeau et al., 2014), and oxidoreductases could help aphids to cope with these
453 secondary metabolites. Glucose dehydrogenases may similarly help aphids to detoxify defensive
454 compounds of the host-plant (Carolan et al., 2011; Nicholson et al., 2012).
455 Several proteins orthologous to salivary effectors of *M. persicae* and *A. pisum* have been identified.
456 Likewise, many of the proteins detected in our study (e.g. calcium-binding, DNA-binding, ATP-binding,
457 GTP-binding proteins, glucose dehydrogenases, oxidoreductases, trehalases and phosphatases) have also
458 been previously identified in the saliva of different aphid species, which were not gall-inducers (Harmel
459 et al., 2008; Nicholson et al., 2012; Elzinga & Jander, 2013; Vandermoten et al., 2014). Therefore,
460 although these proteins probably contribute to plant manipulation by aphids (Elzinga & Jander, 2013),
461 they are probably not specifically involved in gall induction. Interestingly, calcium-binding proteins are
462 supposedly key components of sap-feeding aphids' saliva, preventing the plugging of sieve tubes (Will et
463 al., 2007). Since *P. passerinii* does not feed on sap (Pointeau et al., 2012), it suggests that these proteins
464 also play other crucial roles during aphid-plant interactions. Several proteins detected in the saliva of *P.*
465 *passerinii* such as serine proteases, acid phosphatases, lipases and metalloproteases have been proposed
466 as potential effectors involved in formation and/or maintenance of fig wasps galls (Martinson, Hackett,
467 Machado & Arnold, 2015).
468 *In situ* biochemical assays confirmed the presence of peroxidases in both solid and soluble saliva of *P.*
469 *passerinii*. The phenoloxidase activity is also congruent with the numerous oxidoreductase sequences

identified in the salivary transcriptome. Likewise, the absence of pectin (methyl) esterase and polygalacturonase activity during *in situ* bioassays is consistent with their absence in the salivary transcriptome. However, while numerous proteases were identified among the salivary proteins of *P. passerin*ii, no activity was observed during *in situ* bioassays. Gelatin was probably not the adequate substrate to detect the protease activity of *P. passerinii*. Additional *in situ* assays could be conducted to detect, in *P. passerinii* saliva, the activity of the proteases and possibly other enzymes like cellulases (Cherqui & Tjallingii, 2000). A proteomic analysis of salivary extracts should also confirm and complement the predictions of our transcriptomic approach (Carolan et al., 2011; Boulain et al., 2018).

To knock-down or divert stress signaling and/or ensure finely-tuned reprogramming of host metabolism and anatomical transformation of host tissues, plant manipulation by herbivores or pathogens generally requires reconfiguration of phytohormone pathways and signaling (Giron, Frago, Glevarec, Pieterse & Dicke, 2013; Tooker & Helms, 2014). Both RT-qPCR experiments and histochemical assays confirmed that *P. passerinii* can actively manipulate phytohormone pathways during compatible interactions. This is in line with the numerous proteins potentially interfering with plant signaling and metabolism found in the aphid saliva. Salivary extracts of *P. passerinii* did not affect the auxin biosynthesis during compatible interactions, but downregulated auxin transporter genes such as *PtPIN1* and *PtAUX1*, as well as *PtGH3*, which is involved in the homeostasis of auxin active forms (Park et al., 2007). These downregulations could lead to intracellular accumulation of active auxin forms, and result in the targeted cell hypertrophy and multiplication commonly observed during gall differentiation by *P. passerinii* (Dardeau et al., 2014). The activation of the auxin-responsive promoter *IAA2* during *in planta* assays with transgenic seedlings of *A. thaliana* further supports this hypothesis of an intracellular accumulation of auxin during gall initiation by *P. passerinii*. Similar auxin accumulation, as a result of a reduction in both *PtGH3* activity and auxin transport, is also probably involved in the initiation and development of root galls by cyst and root-

494 knot nematodes (Karczmarek, Overmars, Helder & Goverse, 2004), suggesting a potentially convergent
495 manipulation strategy between these organisms. As genes related to cytokinin biosynthesis (*PtIPT*) and
496 activation (*PtLOG5*) were not affected by salivary proteins of *P. passerinii*, the strong downregulation of
497 cytokinin signaling genes (*PtAHK4*, *PtARR2* and *PtARR16*) upon treatment could correspond to an auxin
498 accumulation-induced regulation loop (Jones et al., 2010; Schaller, Bishopp, & Kieber, 2015). In this
499 aspect, *P. passerinii* could manipulate auxin and cytokinin plant responses to promote the host division
500 cycle leading to the formation of galls (Giron et al., 2013), which provide to the insects food and shelter
501 at the expense of the host plant (Tooker & De Moraes, 2008).
502
503 Apart from the Mp10 effector, the saliva of *P. passerinii* and *M. persicae* shared few similarities. The
504 transcriptomes of *P. passerinii* and *M. persicae* have been obtained with a different sequencing and
505 assembly methods (Ramsay et al., 2007). This probably explains the difference in transcripts amounts
506 gathered for both aphids and several salivary proteins of *M. persicae* might be missing in its
507 transcriptome, leading to an apparently low similarity between secretomes. Previous comparisons
508 among salivary proteins of aphid species also indicated that aphids with different host species and / or
509 feeding strategies exhibited very different salivary protein profiles (Cooper, Dillwith & Puterka, 2011;
510 Vandermoten et al., 2014). This is in agreement with the highly significant effect of aphid species on
511 gene expression profiles in both poplar genotypes. Nonetheless, gene expression profiles of poplar
512 protoplasts during incompatible interactions shared many similarities with those observed during non-
513 host interactions. Both types of interactions were characterized by an overall upregulation of host genes,
514 which was generally more important during non-host interactions than during incompatible ones,
515 probably because one of the three biological replicates of incompatible interactions shared similarities
516 with compatible interactions. During both non-host and incompatible interactions, most genes involved
517 in jasmonates, ethylene and salicylic acid pathways were upregulated. All of these pathways can be

518 activated following aphid feeding, together or separately, depending on the aphid – plant interaction
519 system considered (Morkunas, Mai & Gabryś, 2011; Kerchev, Fenton, Foyer & Hancock, 2012; Louis &
520 Shah, 2013). Due to the salicylic acid - jasmonates cross-talk, a differential gene expression between the
521 two pathways could be expected (Zarate, Kempema & Walling, 2007), but was not observed here.
522 However, this may occur later during the interaction, since in our experiments we only considered early
523 gene responses (Kerchev et al., 2012). As a consequence of activation of plant defense signaling, genes
524 related to secondary metabolism, i.e. *PtF3'5'H, PtANT* and *PtF5H* were also upregulated during both
525 incompatible and non-host interactions, while they were unaffected or downregulated during
526 compatible interactions. This is in agreement with previous histochemical analyses showing a light and
527 transient accumulation of phenolic compounds followed by their marked disappearance in galled tissues
528 during a compatible interaction, while their accumulation was strong and continuous during an
529 incompatible interaction (Dardeau et al., 2014).
530 Interestingly, most of the few genes that were differentially expressed during non-host and incompatible
531 interactions were related to biotic stress signaling, and all genes but *PtJAZ1* were upregulated during
532 incompatible interactions while they were unaffected or downregulated during non-host interactions.
533 These genes included ROS-related genes, *PtSOD* and *PtCAT*, the expression of which was slightly
534 downregulated during non-host interactions. A similar repression of *SOD* and *CAT* genes, leading to an
535 increase in H_2O_2 content, together with an upregulation of *JAZ1* and *PR1*, has been reported in potato
536 leaves infested by *M. persicae* (Kerchev et al., 2012). Some phytohormones-related genes were also
537 upregulated during incompatible interactions only, like *PtAOS* for jasmonates, *PtPR5* for salicylic acid,
538 *PtLOG5* for cytokinins, *PtNIT1* for auxin, and finally *PtEIN2* for ethylene. This latter gene is involved in
539 transduction of ethylene signaling and can be up- or downregulated during both compatible and
540 incompatible interactions in different plant-aphid systems and plays equivocal roles during host-plant
541 resistance to *M. persicae* (Morkunas et al., 2011; Louis & Shah, 2013). Moreover, the putative

intracellular accumulation of auxin during compatible interactions could also interfere with salicylic acid signaling and defense responses (Park et al., 2007), which is congruent with the overall downregulation of salicylic acid pathway related genes. The downregulation of *PtAHK4* and *PtARR2* could also interfere with stress signaling by preventing both accumulation of jasmonates and activation of *PtPR1* (O'Brien & Benkova, 2013), which is consistent with our observations during compatible interactions. As a result, the effectors of *P. passerinii* saliva, in addition to modifying phytohormonal contents, down-regulate the plant defenses to allow gall formation.

In conclusion, our transcriptomic analysis of the saliva of *P. passerinii* and *M. persicae* showed that the gall-inducing aphid probably secretes a highly peculiar saliva, filled with potential effectors that may interfere with several plant secondary messengers and signaling pathways. Our *in vivo* and *in planta* approaches confirmed the ability of salivary extracts of the gall-inducing insects to manipulate host response during compatible interactions. As expected phytohormones pathways were strongly affected, probably to impair biotic stress signaling but also to reconfigure host metabolism and anatomy. Although the saliva of *P. passerinii* and *M. persicae* were very different, incompatible and non-host interactions led to similar host responses, with a different intensity however, and few differences in biotic stress signaling. Additional modalities including different populations of *P. passerinii*, different poplar genotypes with intermediate resistance levels, leading for instance to semi-compatible interactions, and additional host metabolic pathways could be considered in future experiments and give further insights on the molecular processes underpinning failed and successful host manipulation by a gall-inducer.

References

Arvidsson S., Kwasniewski M., Riaño-Pachón D.M. & Mueller-Roeber B. (2008). QuantPrime--a flexible

566 tool for reliable high-throughput primer design for quantitative PCR. *BMC Bioinformatics*, 9, 465.

567 Atamian H.S., Chaudhary R., Dal Cin V., Bao E., Girke T. & Kaloshian I. (2013) *In planta* expression or
568 delivery of potato aphid *Macrosiphum euphorbiae* effectors Me10 and Me23 enhances aphid fecundity.
569 *Molecular Plant-Microbe Interactions*, 26, 67–74.

570 Bendtsen J.D., Jensen L.J., Blom N., Von Heijne G. & Brunak, S. (2004). Feature-based prediction of non-
571 classical and leaderless protein secretion. *Protein Engineering Design and Selection*, 17, 349-356.

572 Bishopp A., El-Showk S., Weijers D., Scheres B., Friml J., Benková E., … Helariutta Y. (2011). A mutually
573 inhibitory interaction between auxin and cytokinin specifies vascular pattern in roots. *Current Biology*,
574 21, 917-926.

575 Boulain H., Legeai F., Guy E., Morlière S., Douglas N.E., Oh J., ... & Sugio A. (2018). Fast evolution and
576 lineage-specific gene family expansions of aphid salivary effectors driven by interactions with host-
577 plants. *Genome Biology and Evolution*, 10, 1554-1572.

578 Buerkner P.C. (2016) brms: An R package for Bayesian multilevel models using Stan. *Journal of Statistical*
579 *Software*, 80, 1-28.

580 Carolan J.C., Fitzroy C.I.J., Ashton P.D., Douglas A.E. & Wilkinson T.L. (2009). The secreted salivary
581 proteome of the pea aphid *Acyrthosiphon pisum* characterised by mass spectrometry. *Proteomics*, 9,
582 2457–2467.

583 Carolan J.C., Caragea D., Reardon K.T., Mutti N.S., Dittmer N., … Edwards O.R. (2011). Predicted effector
584 molecules in the salivary secretome of the pea aphid (*Acyrthosiphon pisum*): a dual
585 transcriptomic/proteomic approach. *Journal of Proteome Research*, 10, 1505–1518.

586 Chaudhary R., Atamian H.S., Shen Z., Briggs S.P. & Kaloshian I. (2014). GroEL from the endosymbiont
587 *Buchnera aphidicola* betrays the aphid by triggering plant defense. *Proceedings of the National Academy*
588 *of Sciences*, 111, 8919-8924.

589 Cherqui A. & Tjallingii W.F. (2000). Salivary proteins of aphids, a pilot study on identification, separation
590 and immunolocalisation. *Journal of Insect Physiology*, 46, 1177–1186.
591 Conesa A., Götz S., García-Gómez J.M., Terol J., Talón M. & Robles M. (2005). Blast2GO: a universal tool
592 for annotation, visualization and analysis in functional genomics research. *Bioinformatics*, 21, 3674–
593 3676.
594 Cooper W.R., Dillwith J.W. & Puterka G.J. (2011). Comparisons of salivary proteins from five aphid
595 (Hemiptera: Aphididae) species. *Environmental Entomology*, 40, 151-156.
596 Dardeau F., Deprost E., Laurans F., Lainé V., Lieutier F. & Sallé, A. (2014). Resistant poplar genotypes
597 inhibit pseudogall formation by the wooly poplar aphid, *Phloeomyzus passerinii* Sign. *Trees*, 28, 1007-
598 1019.
599 De Vos M. & Jander G. (2009). *Myzus persicae* (green peach aphid) salivary components induce defence
600 responses in *Arabidopsis thaliana*. *Plant Cell & Environment*, 32, 1548–1560.
601 Elzinga D.A. & Jander G. (2013). The role of protein effectors in plant–aphid interactions. *Current Opinion*
602 *in Plant Biology*, 16, 451-456.
603 Emanuelsson O., Nielsen H., Brunak S. & von Heijne G. (2000). Predicting subcellular localization of
604 proteins based on their N-terminal amino acid sequence. *Journal of Molecular Biology*, 300, 1005-1016.
605 Favery B., Quentin M., Jaubert-Possamai S. & Abad P. (2016). Gall-forming root-knot nematodes hijack
606 key plant cellular functions to induce multinucleate and hypertrophied feeding cells. *Journal of insect*
607 *physiology*, 84, 60-69.
608 Giron D., Frago E., Glevarec G., Pieterse C.M. & Dicke M. (2013). Cytokinins as key regulators in plant–
609 microbe–insect interactions: connecting plant growth and defence. *Functional Ecology*, 27, 599-609.
610 Giron D., Huguet E., Stone G.N. & Body M. (2016). Insect-induced effects on plants and possible effectors
611 used by galling and leaf-mining insects to manipulate their host-plant. *Journal of Insect Physiology*, 84,
612 70-89.

613 Guiguet A., Dubreuil G., Harris M.O., Appel H., Schultz J.C., Pereira M.H. & Giron D. (2016). Shared
614 weapons of blood- and plant-feeding insects: surprising commonalities for manipulating hosts. *Journal of*
615 *Insect Physiology*, 84, 4–21.
616 Guo K., Wang W., Luo L., Chen J., Guo Y. & Cui F. (2014). Characterization of an aphid-specific, cysteine-
617 rich protein enriched in salivary glands. *Biophysical Chemistry*, 189, 25–32.
618 Harmel N., Létocart E., Cherqui A., Giordanengo P., Mazzucchelli G., Guillonneau F., … Francis F. (2008).
619 Identification of aphid salivary proteins: a proteomic investigation of *Myzus persicae*. *Insect Molecular*
620 *Biology*, 17, 165–174.
621 Hogenhout S.A. & Bos J.I. (2011). Effector proteins that modulate plant–insect interactions. *Current*
622 *Opinion in Plant Biology*, 14, 422-428.
623 Hyatt D., Chen G.L., LoCascio P.F., Land M.L., Larimer F.W. & Hauser L.J. (2010). Prodigal: prokaryotic
624 gene recognition and translation initiation site identification. *BMC Bioinformatics*, 11:119.
625 Jaouannet M., Rodriguez P.A., Thorpe P., Lenoir C.J.G., MacLeod R., Escudero-Martinez C. & Bos J.I.B.
626 (2014). Plant immunity in plant–aphid interactions. *Frontiers in Plant Science*, 5, 663.
627 Ji R., Yu H., Fu Q., Chen H., Ye W., Li S. & Lou Y. (2013). Comparative transcriptome analysis of salivary
628 glands of two populations of rice brown planthopper, *Nilaparvata lugens*, that differ in virulence. *PloS*
629 *one*, 8, e79612.
630 Jones B., Gunnerås S.A., Petersson S.V., Tarkowski P., Graham N., May S., … Ljung, K. (2010). Cytokinin
631 regulation of auxin synthesis in *Arabidopsis* involves a homeostatic feedback loop regulated via auxin and
632 cytokinin signal transduction. *The Plant Cell*, 22, 2956-2969.
633 Jones P., Binns D., Chang H.Y., Fraser M., Li W., McAnulla C., ... Pesseat S. (2014). InterProScan 5:
634 genome-scale protein function classification. *Bioinformatics*, 30, 1236-1240.

635 Karczmarek A., Overmars H., Helder J. & Goverse A. (2004). Feeding cell development by cyst and
636 root-knot nematodes involves a similar early, local and transient activation of a specific auxin-inducible
637 promoter element. *Molecular Plant Pathology*, 5, 343-346.

638 Kerchev P.I., Fenton B., Foyer C.H. & Hancock R.D. (2012). Infestation of potato (*Solanum tuberosum* L.)
639 by the peach-potato aphid (*Myzus persicae* Sulzer) alters cellular redox status and is influenced by
640 ascorbate. *Plant, Cell & Environment*, 35, 430-440.

641 Lieutier F., Bermudez-Torres K., Cook J., Harris M.O., Legal L., Sallé A., … Giron D. (2017). From Plant
642 Exploitation to Mutualism (eds N. Sauvion, D. Thiéry & P. A. Calatayud), pp. 55-109. Elsevier.

643 Louis J. & Shah J. (2013). *Arabidopsis thaliana—Myzus persicae* interaction: shaping the understanding of
644 plant defense against phloem-feeding aphids. *Frontiers in Plant Science*, 4, 213.

645 Malamy J.E. & Benfey P.N. (1997). Organization and cell differentiation in lateral roots of *Arabidopsis*
646 *thaliana*. *Development*, 124, 33-44.

647 Martinson E.O., Hackett J.D., Machado C.A. & Arnold A.E. (2015). Metatranscriptome analysis of fig
648 flowers provides insights into potential mechanisms for mutualism stability and gall induction. *PloS One*,
649 10, e0130745.

650 Morkunas I., Mai V.C. & Gabryś B. (2011). Phytohormonal signaling in plant responses to aphid feeding.
651 *Acta Physiologia Plantarum*, 33, 2057–2073.

652 Mutti N.S., Louis J., Pappan L.K., Pappan K., Begum K., Chen M.S., … Reeck G.R. (2008). A Protein from the
653 salivary glands of the pea aphid, *Acyrthosiphon pisum*, is essential in feeding on a host plant. *Proceedings*
654 *of the National Academy of Sciences*, 105, 9965-9969.

655 Nicholson S.J., Hartson S.D. & Puterka G.J. (2012). Proteomic analysis of secreted saliva from Russian
656 Wheat Aphid (Diuraphis noxia Kurd.) biotypes that differ in virulence to wheat. *Journal of Proteomics*, 75,
657 2252–2268.

658 O'Brien J.A. & Benková E. (2013). Cytokinin cross-talking during biotic and abiotic stress responses.
659 *Frontiers in Plant Science*, 4, 451.

660 Oksanen J., Blanchet F.G., Kindt R., Legendre P., Minchin P.R., O'hara R.B., … Wagner H. (2013). Package
661 'vegan'. Community Ecol Package Version 2.

662 Pan Y., Zhu J., Luo L., Kang L. & Cui F. (2015). High expression of a unique aphid protein in the salivary
663 glands of *Acyrthosiphon pisum*. *Physiological and Molecular Plant Pathology*, 92, 175–180.

664 Park J.E., Park J.Y., Kim Y.S., Staswick P.E., Jeon J., Yun J., … Park C.M. (2007). GH3-mediated auxin
665 homeostasis links growth regulation with stress adaptation response in *Arabidopsis*. *Journal of Biological*
666 *Chemistry*, 282, 10036–10046.

667 Petersen T.N., Brunak S., von Heijne G. & Nielsen H. (2011). SignalP 4.0: discriminating signal peptides
668 from transmembrane regions. *Nature Methods*, 8, 785.

669 Pierleoni A., Martelli P.L. & Casadio, R. (2008). PredGPI: a GPI-anchor predictor. *BMC Bioinformatics*, 9,
670 392.

671 Pointeau S., Ameline A., Laurans F., Sallé A., Rahbé Y., Bankhead-Dronnet S. & Lieutier F. (2012).
672 Exceptional plant penetration and feeding upon cortical parenchyma cells by the woolly poplar aphid.
673 *Journal of Insect Physiology*, 58, 857–866.

674 Pundir S., Martin M.J. & O'Donovan C. (2017). Uniprot protein knowledgebase. *Protein Bioinformatics:*
675 *From Protein Modifications and Networks to Proteomics*, 41-55.

676 R Core Team (2013). R: A language and environment for statistical computing. R Foundation for
677 Statistical Computing, Vienna, Austria. URL http://www.R-project.org/.

678 Ramsey J.S., Wilson A.C.C., de Vos M., Sun Q., Tamborindeguy C., Winfield A., Malloch G., Smith D.M.,
679 Fenton B., Gray S.M., Jander G. (2007). Genomic resources for *Myzus persicae*: EST sequencing, SNP
680 identification, and microarray design. *BMC Genomics*, 8, 423–423.

681 Sallé A., Pointeau S., Bankhead-Dronnet S., Bastien C. & Lieutier, F. (2017). Unraveling the tripartite
682 interactions among the woolly poplar aphid, its host tree, and their environment: a lead to improve the
683 management of a major tree plantation pest? *Annals of Forest Science*, 74, 79.
684 Schaller G.E., Bishopp A., & Kieber J.J. (2015). The yin-yang of hormones: cytokinin and auxin interactions
685 in plant development. *The Plant Cell*, 27, 44-63.
686 Schoonhoven L.M., Van Loon J.J.A. & Dicke M. (2005). Insect–Plant Biology. Oxford University Press.
687 Schulz M.H., Zerbino D.R., Vingron M. & Birney E. (2012). Oases: robust *de novo* RNA-seq assembly
688 across the dynamic range of expression levels. *Bioinformatics*, 28, 1086-1092.
689 Shorthouse J.D., Wool D., & Raman A. (2005). Gall-inducing insects – nature's most sophisticated
690 herbivores. *Basic and Applied Ecology*, 6, 407-411.
691 Stuart J.J., Chen M.S., Shukle R. & Harris M.O. (2012). Gall midges (Hessian flies) as plant pathogens.
692 *Annual Review of Phytopathology*, 50, 339-357.
693 Testerink C. & Munnik T. (2005). Phosphatidic acid: a multifunctional stress signaling lipid in plants.
694 *Trends in Plant Science*, 10, 368-375.
695 Tong Z., Gao Z., Wang F., Zhou J. & Zhang Z. (2009). Selection of reliable reference genes for gene
696 expression studies in peach using real-time PCR. *BMC Molecular Biology*, 10, 71.
697 Tooker J.F. & De Moraes C.M. (2008). Gall insects and indirect plant defenses: A case of active
698 manipulation? *Plant Signaling & Behavior*, 3, 503-504.
699 Tooker J.F. & Helms A.M. (2014). Phytohormone dynamics associated with gall insects, and their
700 potential role in the evolution of the gall-inducing habit. *Journal of Chemical Ecology*, 40, 742–753.
701 Vandermoten S., Harmel N., Mazzucchelli G., De Pauw E., Haubruge E. & Francis F. (2014). Comparative
702 analyses of salivary proteins from three aphid species. *Insect Molecular Biology*, 23, 67-77.
703 Will T., Tjallingii W.F. Thönnessen A. & van Bel A.J. (2007). Molecular sabotage of plant defense by aphid
704 saliva. *Proceedings of the National Academy of Sciences*, 104, 10536-10541.

705 Wu F.H., Shen S.C., Lee L.Y., Lee S.H., Chan M.T. & Lin C.S. (2009). Tape-*Arabidopsis* Sandwich-a simpler
706 *Arabidopsis* protoplast isolation method. *Plant Methods*, 5, 16.
707 Xue H.W., Chen X. & Mei Y. (2009). Function and regulation of phospholipid signalling in plants.
708 *Biochemical Journal*, 421, 145–156.
709 Yang J.L., Yang R., Cheng A.C., Jia R.Y., Wang M.S. & Zhang S.H. (2010). Five-minute purification of PCR
710 products by new-freeze-squeeze method. *Journal of Food, Agriculture & Environment*, 8, 32–33.
711 Yang Y. & Smith S.A. (2013). Optimizing *de novo* assembly of short-read RNA-seq data for phylogenomics.
712 *BMC Genomics*, 14, 328.
713 Zarate S.I., Kempema L.A. & Walling L.L. (2007). Silverleaf whitefly induces salicylic acid defenses and
714 suppresses effectual jasmonic acid defenses. *Plant Physiology*, 143, 866-875.
715 Zerbino D. & Birney E. (2008). Velvet: algorithms for de novo short read assembly using de Bruijn graphs.
716 *Genome Research*, gr-074492.
717 Zhao C., Escalante L.N., Chen H., Benatti T.R., Qu J., Chellapilla S., … & Richards S. (2015). A massive
718 expansion of effector genes underlies gall-formation in the wheat pest *Mayetiola destructor*. *Current*
719 *Biology*, 25, 613-620.
720 Zhao C., Shukle R., Navarro Escalante L., Chen M., Richards S., & Stuart J.J. (2016). Avirulence gene
721 mapping in the Hessian fly (*Mayetiola destructor*) reveals a protein phosphatase 2C effector gene family.
722 *Journal of Insect Physiology*, 84, 22-31.
723

724 Figure captions

725 Figure 1: Gene Ontology treemap for the salivary transcriptome of *Phloeomyzus passerinii*. The box size
726 correlates to the number of sequences isolated. Numbers between brackets indicate the number of
727 sequences identified. Green boxes indicate binding proteins, purple boxes indicate enzymes, red boxes
728 indicate structural constituents, the blue box indicates transporters and the brown box molecular
729 transducers. A Detailed list of the proteins can be found in the table S4.

730

731 Figure 2: Representative salivary sheaths secreted in artificial diets by *Phloeomyzus passerinii*. Sheaths
732 stained and observed after 24 h probing in an agarose diet: (A) sheath stained with Coomassie blue; (B)
733 black stained sheaths in diet containing 0.1% DOPA, indicating a phenoloxidase activity, note the dark
734 halo surrounding the upper sheath; (C) reddish stained sheath in diet immersed with 0.1% DAB and 0.1%
735 H_2O_2, indicating a peroxidase activity. Black bars represent 10 µm.

736

737 Figure 3: Heatmap of log_2-fold changes of 43 poplar genes belonging to eight different physiological
738 processes or metabolic pathways (lower left box), after incubation of poplar protoplasts of two poplar
739 genotypes (Koster and I-214) with salivary proteins of two aphids (*Myzus persicae* (*M. p.*) and
740 *Phloeomyzus passerinii* (*P. p.*)). Non-host interactions are expected between both poplar genotypes and
741 *M. persicae*, while incompatible interactions are expected between *P. passerinii* and Koster and
742 compatible interactions between *P. passerinii* and I-214. Downregulation appears in blue and
743 upregulation in red. Gene code is presented below the heatmap, modalities (i.e. aphid x poplar genotype
744 combinations are presented on the right of the heatmap). Hierarchical clustering has been built with
745 Euclidean distances.

746 Figure 4: Fold changes of genes involved in auxin (left) and cytokinin (right) pathways of poplar
747 protoplasts collected from two poplar genotypes (I-214 and Koster), after incubation with salivary

748 proteins of two aphids (*Myzus persicae* and *Phloeomyzus passerinii*). Dots represent the average fold
749 change value, and bars represent credibility intervals.

750

751 Figure 5: Representative GUS assays of transgenic seedlings of *Arabidopsis thaliana pIAA2*::GUS, showing
752 whole plants (A, C, E, G, I and K), and root tips (B, D, F, H, J and L), after 3 h of incubation in 20 µM of IAA
753 (A and B), TE/Tween buffer (C and D), and 1 and 10 µg of salivary proteins of *Phloeomyzus passerinii* (E, F,
754 I and J) or *Myzus persicae* (G, H, K and L). Black bars represent 1 mm for whole plants (A, C, E, G, I and K)
755 and 10 µm for root tips (B, D, F, H, J and L). Five seedlings were used for each modality.

756

757 Figure 6: Representative GUS assays of transgenic seedlings of *Arabidopsis thaliana pARR16*::GUS,
758 showing whole plants (A, C, E, G, I and K), and root tips (B, D, F, H, J and L), after 4 h of incubation in 20
759 µM of BAP (A and B), TE/Tween buffer (C and D), and 1 and 10 µg of salivary proteins of *Phloeomyzus*
760 *passerinii* (E, F, I and J) or *Myzus persicae* (G, H, K and L). Black bars represent 1 mm for whole plants (A,
761 C, E, G, I and K) and 10 µm for root (B, D, F, H, J and L). Five seedlings were used for each modality.

762

763

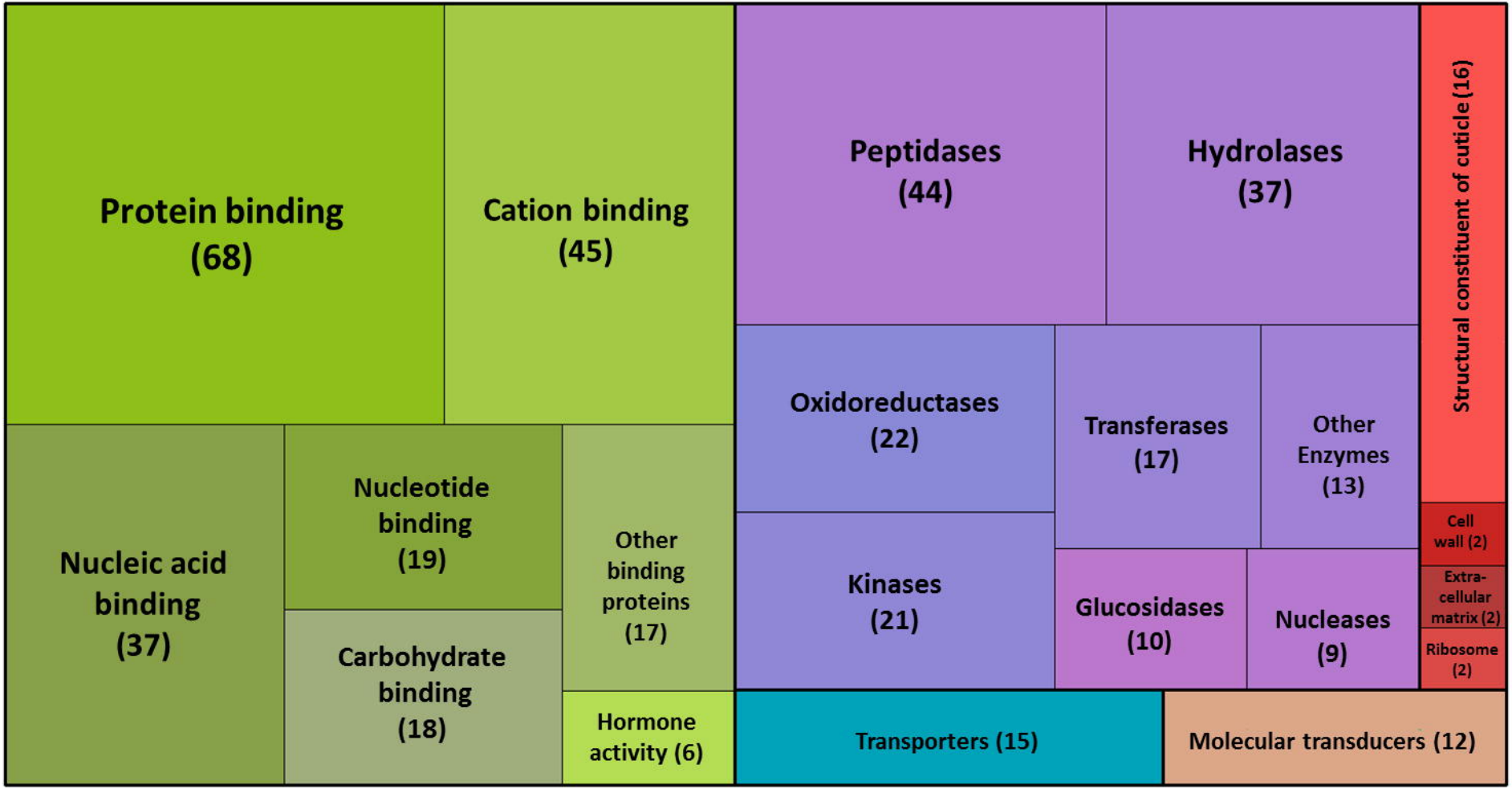
Protein binding (68)
Cation binding (45)
Peptidases (44)
Hydrolases (37)
Structural constituent of cuticle (16)
Oxidoreductases (22)
Transferases (17)
Other Enzymes (13)
Nucleic acid binding (37)
Nucleotide binding (19)
Other binding proteins (17)
Kinases (21)
Glucosidases (10)
Nucleases (9)
Cell wall (2)
Extra-cellular matrix (2)
Carbohydrate binding (18)
Ribosome (2)
Hormone activity (6)
Transporters (15)
Molecular transducers (12)

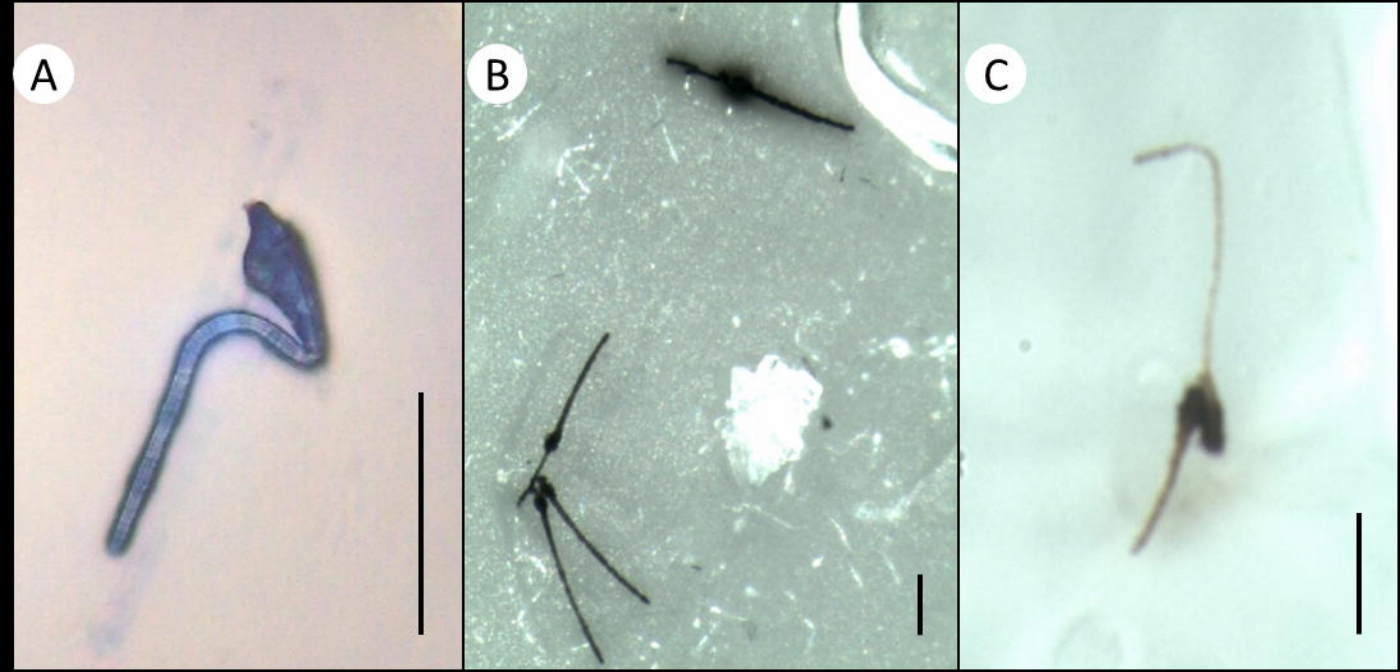
A
B
C

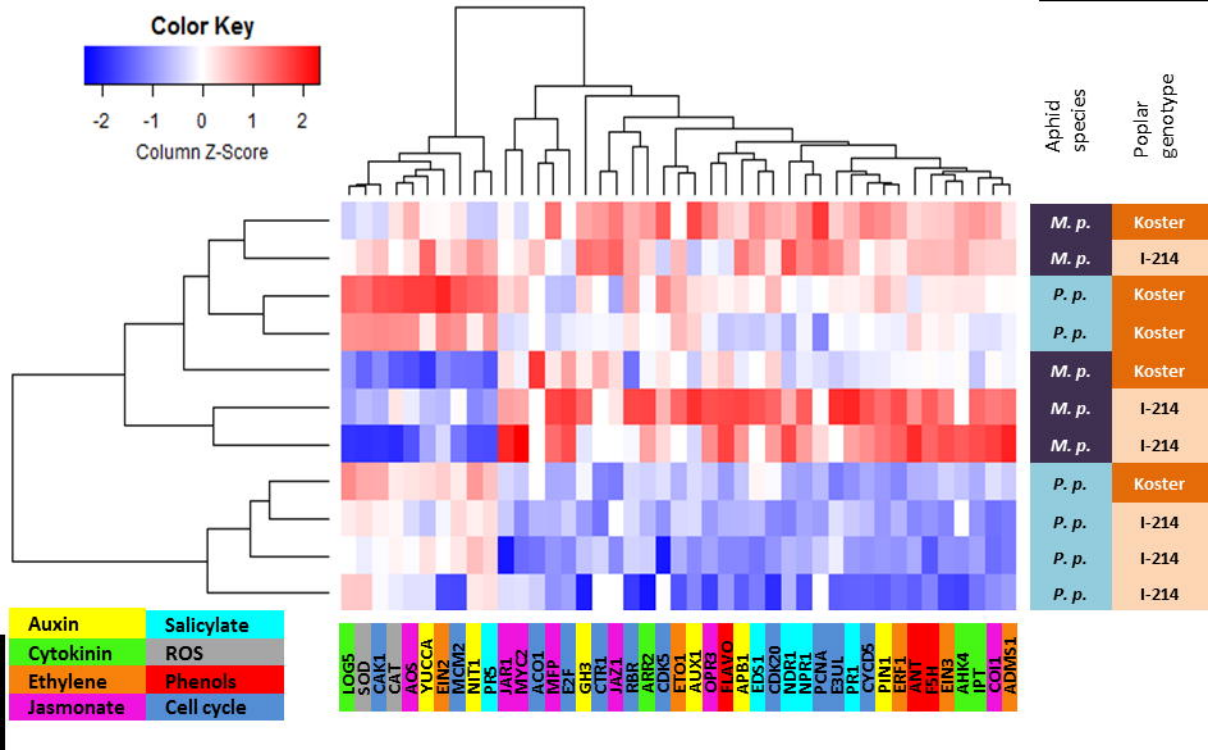
Color Key
-2
-1
0
1
2
Column Z-Score
Aphid species
Poplar genotype
M. p.
Koster
M. p.
I-214
P. p.
Koster
P. p.
Koster
M. p.
Koster
M. p.
I-214
M. p.
I-214
P. p.
Koster
P. p.
I-214
P. p.
I-214
P. p.
I-214
Auxin
Salicylate
Cytokinin
ROS
Ethylene
Phenols
Jasmonate
Cell cycle
LOG5
SOD
CAK1
CAT
AOS
YUCCA
EIN2
MCM2
NIT1
PIB
JAR1
MYC2
ACO1
MFP
E2F
GH3
CTR1
JAZ1
RBR
ARR2
CDKB
ETO1
AUX1
OPR3
FLAVO
APB1
EDS1
CDK20
NDR1
NPR1
PCNA
E3UL
PR1
CYCD5
PIN1
ERF1
ANT
F5H
EIN3
AHK4
IPT
COI1
ADMS1

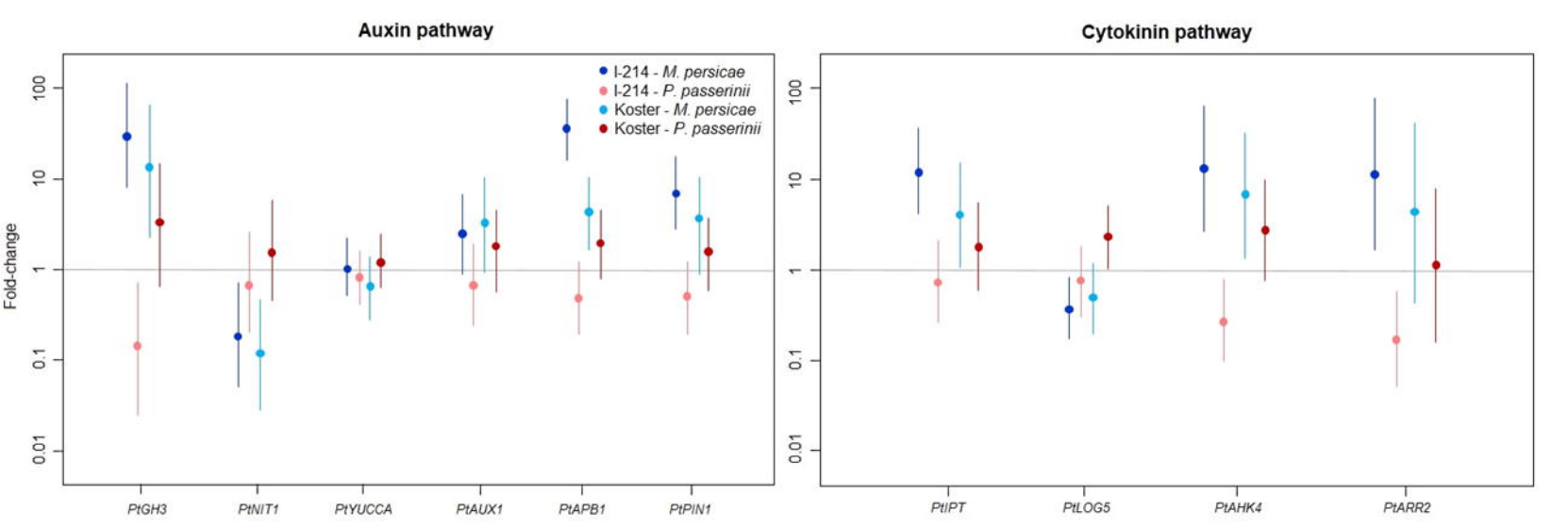
Auxin pathway
Cytokinin pathway
I-214 - M. persicae
I-214 - P. passerinii
Koster - M. persicae
Koster - P. passerinii
Fold-change
100
10
1
0.1
0.01
PtGH3
PtNIT1
PtYUCCA
PtAUX1
PtAPB1
PtPIN1
PtIPT
PtLOG5
PtAHK4
PtARR2

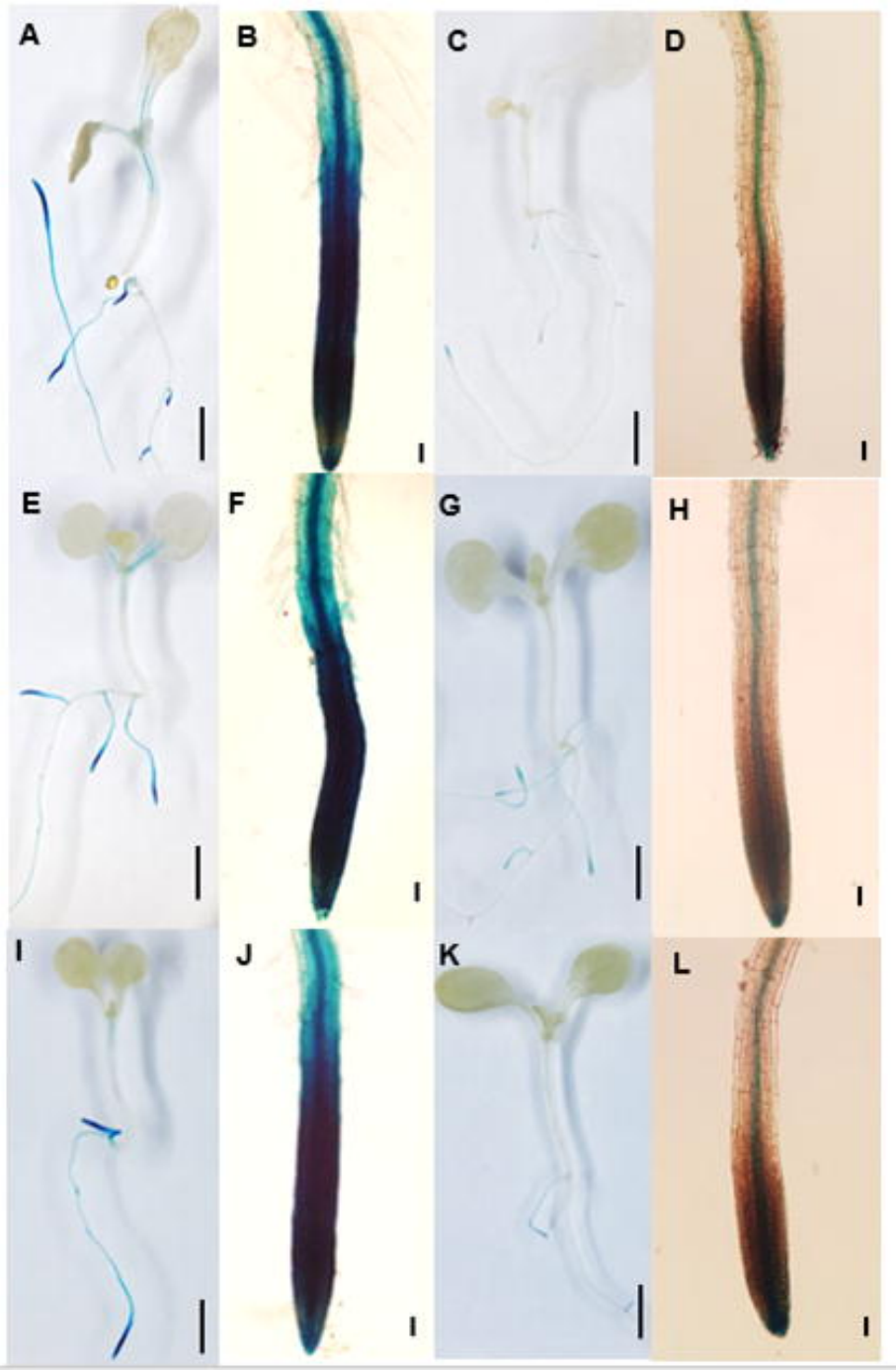
A
B
C
D
E
F
G
H
I
J
K
L

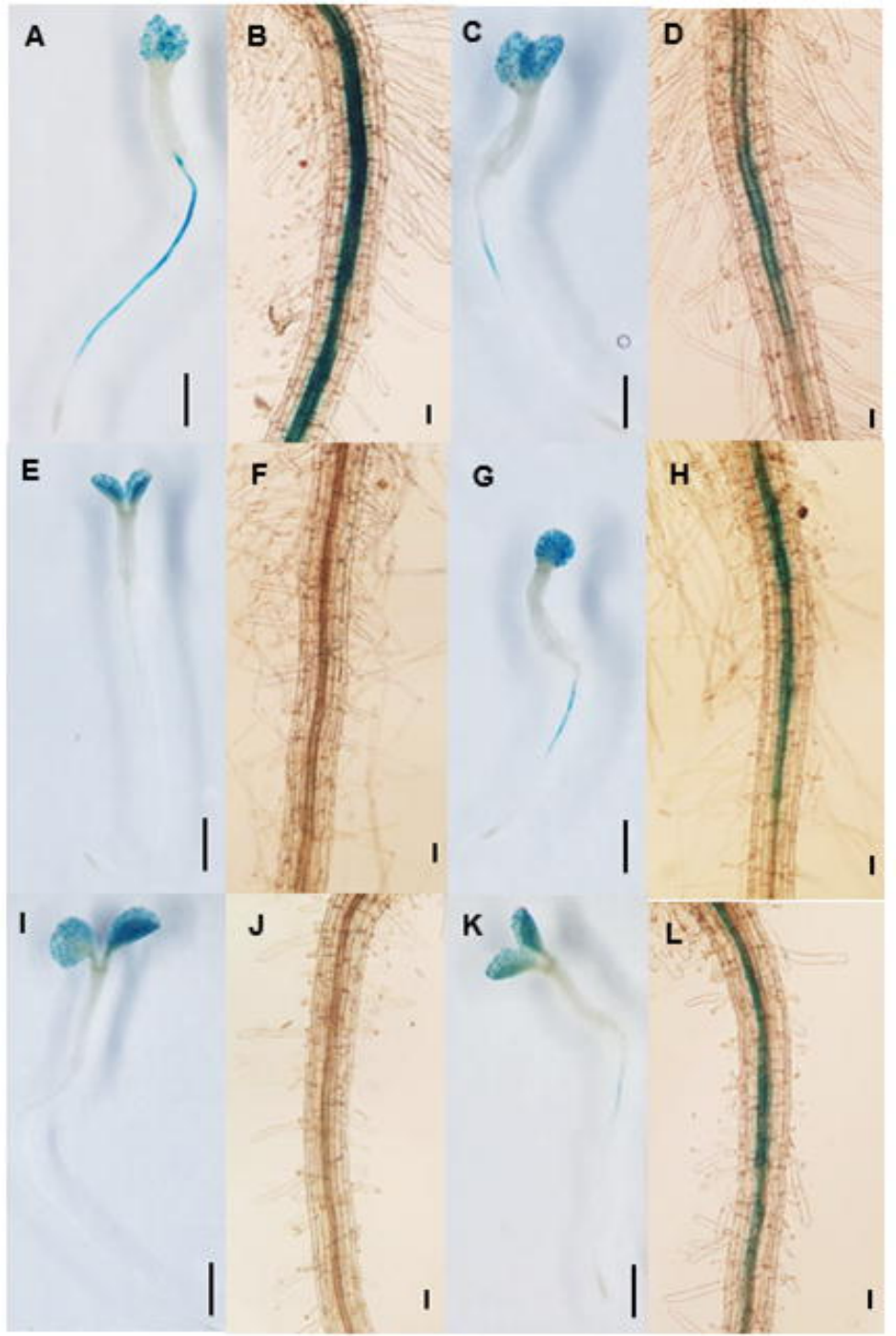
A
B
C
D
E
F
G
H
I
J
K
L